Advances in Science and Technology Research Journal

Advances in Science and Technology Research Journal, 2025, 19(6), 403–413
https://doi.org/10.12913/22998624/203459
ISSN 2299-8624, License CC-BY 4.0

Received: 2025.02.20
Accepted: 2025.04.15
Published: 2025.05.01

Study of the behavior of thin-walled composite structures with closed sections under three-point bending tests

Patryk Różyło[1]

[1] Department of Machine Design and Mechatronics, Faculty of Mechanical Engineering, Lublin University of Technology, Nadbystrzycka 36, 20-618 Lublin, Poland
E-mail: p.rozylo@pollub.pl

ABSTRACT

Thin-walled composite columns with a closed rectangular cross-section are the subject of this study. The test specimens were made using the autoclave technique and were characterized by constant geometric parameters. Experimental tests were carried out using interdisciplinary techniques within the framework of experimental testing, which enabled an in-depth analysis of the bending behavior of the composite structures. The research analyzed the effect of varying boundary conditions (support spacing) on the load carrying capacity of the structure and the damage state of the composite. In the course of the research, the damage phenomenon was evaluated both quantitatively and qualitatively. The aim of the study was to investigate the load-carrying capacity of thin-walled composite structures subjected to bending using interdisciplinary experimental testing methods, including non-destructive methods. The novelty of the study was mainly the preliminary demonstration of a research approach to assessing the limit states of a bending structure in terms of changes in boundary conditions – support spacing.

Keywords: thin-walled columns, failure, three-point bending, experimental study.

INTRODUCTION

Thin-walled composite structures are a special group of load-carrying structures, widely used in a broad range of industries. The wide range of applications of such structures determines advanced research in the context of their proper exploitation - especially in conditions where it is important to maintain a significant level of strength of the structure under external loads [1–3]. Composite structures are a group of structures characterized by the special property of keeping their own weight low while maintaining high strength. Most researchers have so far dealt with the phenomenon of stability and load-carrying capacity analyses of composite structures under (usually axial) compression in a very broad manner. Studies in the field of limit state testing under compressive loads have focused primarily on the phenomenon of loss of stability (buckling), damage initiation, etc. [4–6]. Structures of the aforementioned type are most often subjected to external loads causing axial and eccentric compression [7–10], or bending [11–12]. The study of stability and load-carrying capacity in compression of thin-walled composite profiles has been described quite extensively in recent years by the authors of many research papers [13–16]. In general, the studies focused on the examination of the structure's behavior in a critical state (when there was a loss of stability), the damage phase due to further axial loading of the structure, and the analysis of the first signs of damage, such as fiber/matrix damage or delamination. All of the above, regardless of the cross-sectional shape of the composite structures, was analyzed mainly in the context of tests where the structures were compressed. An important issue from the perspective of static testing is, in addition to the axial and eccentric compression widely described in the literature, also bending of this type of profiles - which is the subject of consideration in this

paper [17–20]. The phenomenon of bending of thin-walled composite structures with open and closed sections is still a current issue and requires thorough research. It is necessary to have an interdisciplinary approach in conducting research activities – especially using advanced methods of experimental research, as well as numerical simulations [16, 21–23]. The basic apparatus for conducting static bending tests is, as in most cases, a universal testing machine. Additional support through such systems as digital image correlation apparatus, a device for analyzing acoustic emission signals, and digital microscopy enable detailed evaluation of the phenomenon of loss of load-carrying capacity of structures made of composite materials subjected to bending. Examples of the use of the aforementioned research devices are presented in papers [23–26]. It is important to take a future approach to research on composite materials - including the use of biocomposites, as widely described in the papers [27,28]. Regardless of the available research on the phenomenon of bending thin-walled composite structures, an in-depth research on this topic requires further investigation, especially in the context of determining the dominant causes of loss of structural load-carrying capacity as well as investigations involving the impact of boundary conditions (e.g. support spacing for load-carrying capacity) and the influence of the shape of the cross-section or the composite ply arrangement (lay-up) on the limit states in static bending tests. In this paper, the impact of changes in boundary conditions - support spacing – on the load-carrying capacity of thin-walled CFRP structures was investigated using independent research methods, including non-destructive testing.

Subject and methodology od research

The subjects of the study were thin-walled columns made of CFRP composite material. The test profiles were characterized by identical geometric parameters and were manufactured using the autoclave technique. Material parameters were determined in accordance with standards for static determination of properties of composite materials: PN-EN ISO 527-5 [29] (ASTM D 3039 [30]), PN-EN ISO 14129 [31] (ASTM D 3518 [32]), PN-EN ISO 14126 [33] (ASTM D 3410 [34]). The material parameters are presented in detail in the paper [35]. The material properties of the composite were presented in Table 1. The detailed method for determining material properties in the case of analyzed composite structures is presented in the papers [36, 37].

The composite structures consisted of 8 layers of equal thickness, where the total thickness of the structure was 1.24 mm. The lay-up of the laminates used for the tests was characterized by a symmetrical arrangement of individual layers $[0°/45°/-45°/90°]_s$. The length of the columns was 200 mm and the internal cross-section was 30 × 50 mm (the thickness of the composite wall was 1.24 mm). More information on the manufactured composite profiles is presented in the papers [23, 24, 35]. The study used three test specimens, as shown in the Figure 1.

The research was conducted using interdisciplinary testing methods. A Cometech QC-505M2F universal testing machine with a load capacity of 50 kN, which is controlled by Amis Plus software, was used. The universal testing machine had special heads mounted for three-point bending. It was possible to register the course of the three-point bending process with the mounted heads, depending on the change in support spacing (distance) – which was the subject of the study of this paper. The tests were conducted at a speed of 2 mm/min under room temperature conditions. The measurable effect of the tests was the generation of load-displacement characteristics. Obviously, the load was registered in the head of the testing machine, while the registered displacement corresponded to the displacement of the crosshead of the testing machine.

In addition, three other testing techniques were used, such as acoustic emission, Aramis 2D optical

Table 1. Determined properties of composite material – average values (with standard deviation)

Mechanical properties		Strength properties	
Young's modulus E_1 (GPa)	103.01 (±2.15)	Tensile strength F_{TU} *(0°)* (GPa)	1.28 (±0.06)
Young's modulus E_2 (GPa)	7.36 (±0.31)	Compressive strength F_{CU} *(0°)* (GPa)	0.57 (±0.05)
Poisson's ratio v_{12} [-]	0.37 (±0.17)	Tensile strength F_{TU} *(90°)* (GPa)	0.03 (±0.01)
Kirchhoff modulus G_{12} (GPa)	4.04 (±0.17)	Compressive strength F_{CU} *(90°)* (GPa)	0.10 (±0.01)
-	-	Shear strength F_{SU} *(45°)* (GPa)	0.13 (±0.01)

Figure 1. Test specimens

deformation measurement system and digital microscopy. For acoustic emission testing, a single-channel SpotWave 201 system (from Vallen) was used, allowing acoustic emission signals to be registered using a dedicated VS150-L piezoelectric sensor. Acoustic emission test parameters were registered using dedicated SpotWave Acquisition software, while analysis of the results was performed in Vallen AE software (as part of the overall Vallen Control Panel package). In the case of the Aramis 2D optical deformation measurement system, deformations of the structure were registered in the measurement surface, where it was possible to visualize defects in the structure using a special median filter. In the case of digital microscopy, the VHX-970F digital microscope (from Keyence) was used, through which the damage of the structure in the area of permanent failure was analyzed. Using the above-mentioned test equipment and software, the level of damage to the composite material was evaluated. In addition to the equilibrium paths determined by testing on the testing machine, the characteristics of selected acoustic emission signals were determined. The above made it possible to assess the phenomenon of damage to composite structures, which was also verified using an optical deformation measurement system and images registered using a digital microscope. The main test stand and additional measuring devices are shown in Figures 2 and 3. Tests were conducted for three different cases of support spacing. The first variant was a case where the

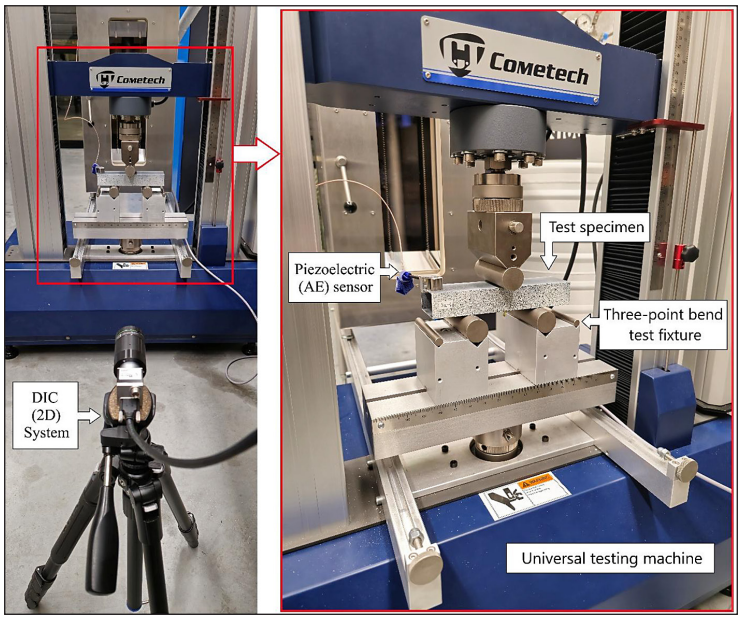

Figure 2. Main test stand

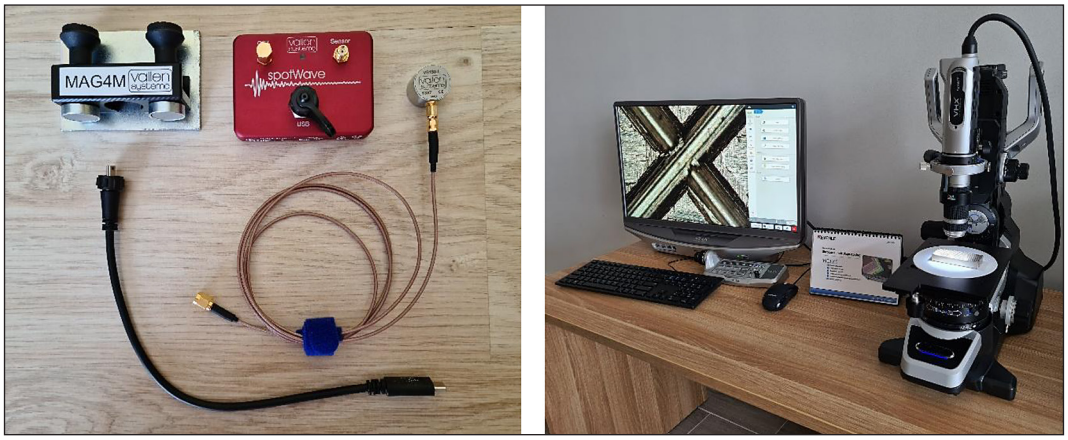

Figure 3. Additional measuring devices: single-channel acoustic emission system and digital microscope

support spacing was 100 mm (Sa-1), the second case with a support spacing of 125 mm (Sa-2) and the third was 150 mm (Sa-3). For such three cases, tests were carried out and the effect of changing the boundary conditions – representing a change in the described support spacing – on the course of loading the structure was analyzed. Figure 4 shows the described test conditions.

TEST RESULTS

Based on the research, the load capacity of composite structures was evaluated using the previously mentioned interdisciplinary research methods. The presented research results are preliminary results of research carried out on composite columns with a closed cross-section, using profiles with the same composite material layup as an example, taking into account variable support spacing. Based on the conducted research, equilibrium paths were initially determined, which made it possible to assess the load-carrying capacity of the structure – the load-displacement (displacement of the crosshead) characteristics are presented in the Figure 5.

The load-carrying capacity of the structure was estimated based on the results of static tests,

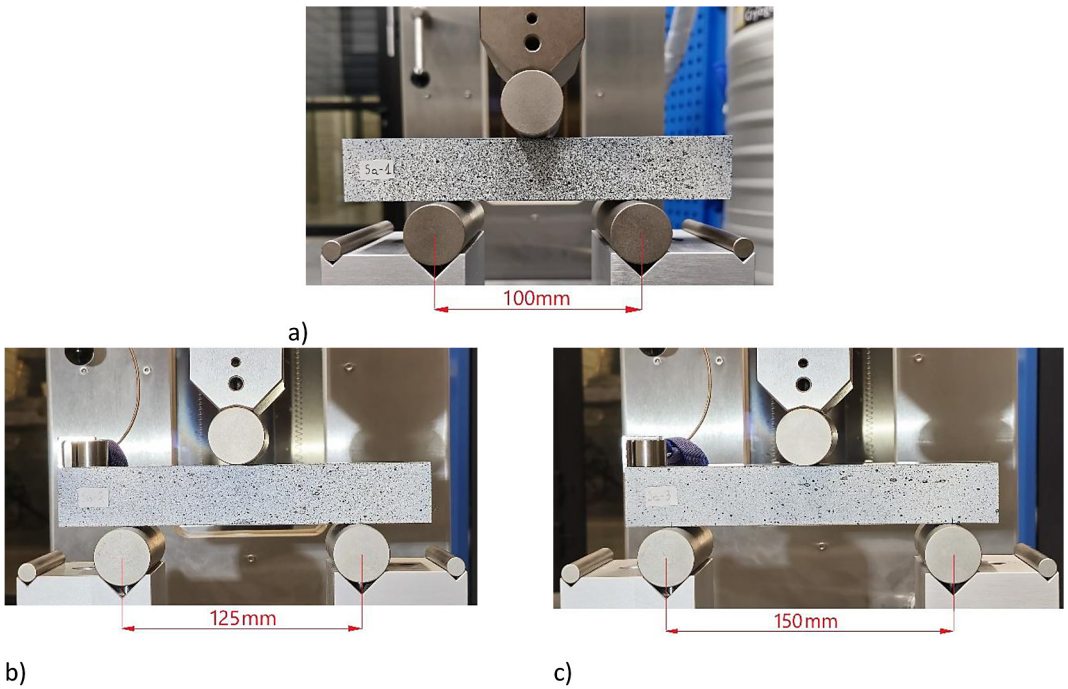

Figure 4. Variable test conditions: a) support spacing of 100 mm (Sa-1), b) support spacing of 125 mm (Sa-2), c) support spacing of 150 mm (Sa-3)

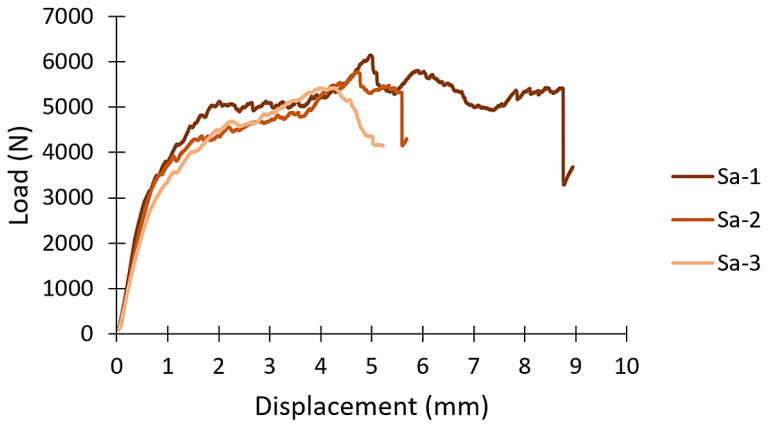

Figure 5. Load-displacement characteristics

in particular three-point bending tests, which were carried out in a range corresponding to the damage of the composite material. The estimated maximum loads made it possible to determine the effect of changing the support spacing on the registered limit force. Based on the tests carried out, it was estimated that the maximum load value was 6144 N (specimen Sa-1), where the support spacing was 100 mm. The limit load value for the second case, where the support spacing was 125 mm, was 5775 N (specimen Sa-2). The lowest ultimate load value was registered in the case of a support distance of 150 mm, where the ultimate load was 5423 N (specimen Sa-3). Obviously, from a research point of view, the above-mentioned trend demonstrates the logic of the registered limit loads, where the load value decreases with the increase of the distance between the supports. Based on the above obtained results of limit loads, the impact of these loads can be estimated depending on the change in the support spacing. The ratio of the maximum load registered for specimen Sa-1 (support spacing 100 mm) compared with specimen Sa-3 (support spacing 150 mm) is 1.13. An important scientific finding was that in the analyzed cases, an almost linear trend was observed in the case of a decrease in the limit load value in relation to an increase in the support spacing - which was demonstrated in Fig. 6. The trendline equation represents a formula that finds the line which best fits the data points. In order to generate a trend line, the function for generating a trend line based on data points in Excel (from Microsoft Office software) was used. The equation of the function describing the trend line and the correlation coefficient of the trend line with the data points were generated automatically.

The high level of linearity of the trend within the registered tendency of a decrease in the limit load in relation to an increase in the value of the support spacing is evidenced by the high correlation coefficient R^2 between the trend line and the experimentally obtained values. The above proves the possible prediction of the behavior of

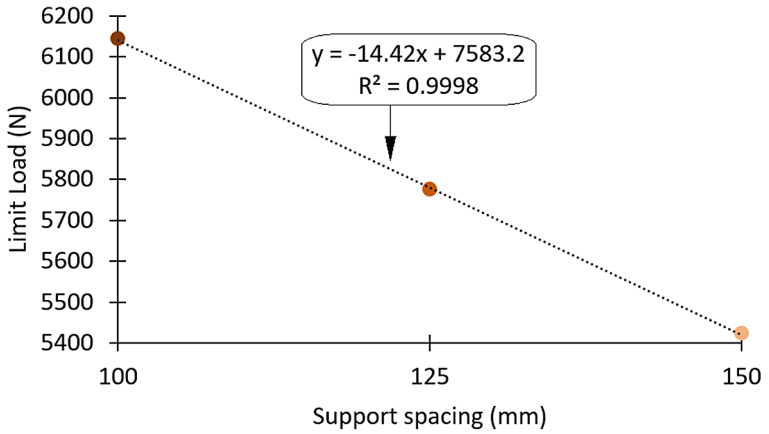

Figure 6. Effect of limit load on the change of support spacing

composite structures in the scope of a variable boundary condition – which in the conducted research was a change in the support spacing. The figure below demonstrates an example of the form of structural failure that occurs with a support spacing of 100 mm (Fig. 7).

Obviously, present research concerns only the composite profiles with the $[0°/45°/-45°/90°]_s$ lay-up - however, the above-observed issue will be verified in further research activities on the example of other lay-ups of the composite material. In the case of experimental studies, several independent additional test methods were used, based on which exemplary results and possibilities for assessing the damage of the composite material are presented. Based on the acoustic emission, additional damage analysis is possible based on the comparison of selected acoustic emission signals with the operating path (load-displacement) of the structure. This paper only presents an example result based on the energy signal within the acoustic emission (Fig. 8).

The results of acoustic emission allow for a more comprehensive assessment of damage to the composite material structure, where local increases in a given acoustic emission signal indicate progressive damage to the structure. An increase in the intensity of the acoustic emission signal (e.g. the energy signal presented) indicates a potentially sudden change in the load-displacement

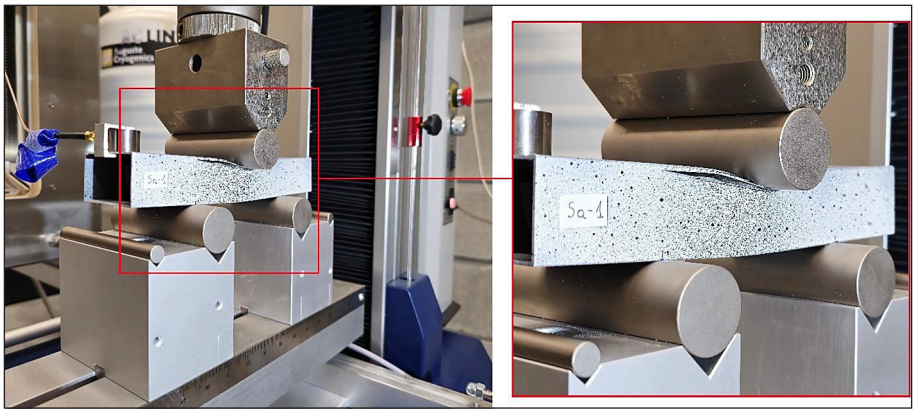

Figure 7. Form of structural damage – specimen Sa-1

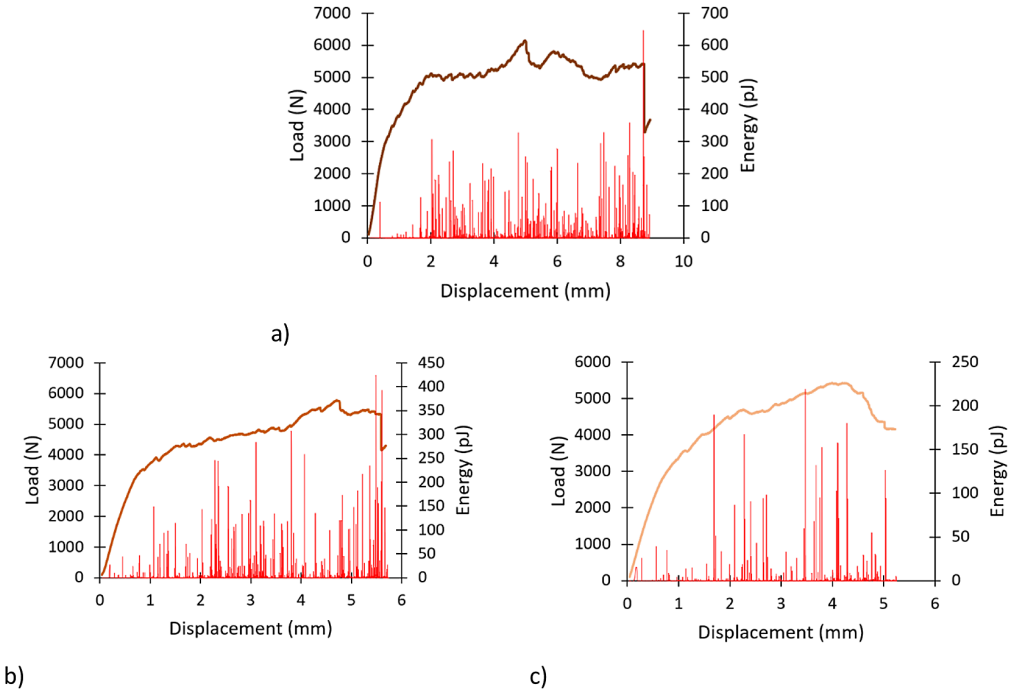

Figure 8. Load-displacement characteristics with acoustic emission energy signal: a) specimen Sa-1, b) specimen Sa-2, c) specimen Sa-3

characteristic. Both the locally occurring "peaks" of acoustic emission signals and their intensity indicate progressive damage, which is well represented by the results shown in Figure 8. It was observed that for specimen Sa-1, the first significant increase in the energy signal occurred at a displacement of 2.03 mm and was approximately 307 pJ. In the case of specimen Sa-2, a similar situation occurred at a displacement of 1.07 mm, where the energy signal was approximately 149 pJ, while for specimen Sa-3, it occurred at a displacement of 1.69 mm, where the energy signal was approximately 190 pJ. Based on the conducted research, it was observed that the damage to thin-walled composite structures is a very complex phenomenon, as evidenced by both the irregularity of the load-displacement curves and the fact that the acoustic emission signal repeatedly increases and decreases. Furthermore, the acoustic emission graphs obtained show that there is a significant change in the density (intensity) of the acoustic emission signal depending on the support spacing – where the signal density is highest at 100 mm support spacing and decreases as the distance between supports increases. This paper does not concentrate on a detailed analysis of the other acoustic emission signals, since this will be the subject of more in-depth research in further scientific investigations on composite profiles with other composite lay-ups. Another important aspect of the research was the use of a method for evaluating the deformation of the composite material structure using digital image correlation technology. By using the 2D optical deformation measurement system, it was possible to estimate the behavior of the structure within the tested area of the composite material. Among other things, the area with the highest strain level was determined (vertical strains were analyzed in relation to the three-point bending). This allowed for a qualitative evaluation of the areas with the highest strain (Fig. 9).

The registered strains (in the vertical direction) allowed for the visualization of critical areas susceptible to damage - where it was observed that the dominant form of damage occurred in each case directly under the element generating the loading of the composite structure. The size of the damage area results from the applied support spacing - where the highest "stiffness" was shown by the first case (Sa-1), and the lowest by the third case (Sa-3), which is confirmed both by the previously presented load-displacement characteristics and local density and "peaks" in the energy signal from acoustic emission, as well as the qualitative results of the structural deformation (strain).

The final technique enabling qualitative estimation of damage to composite material was

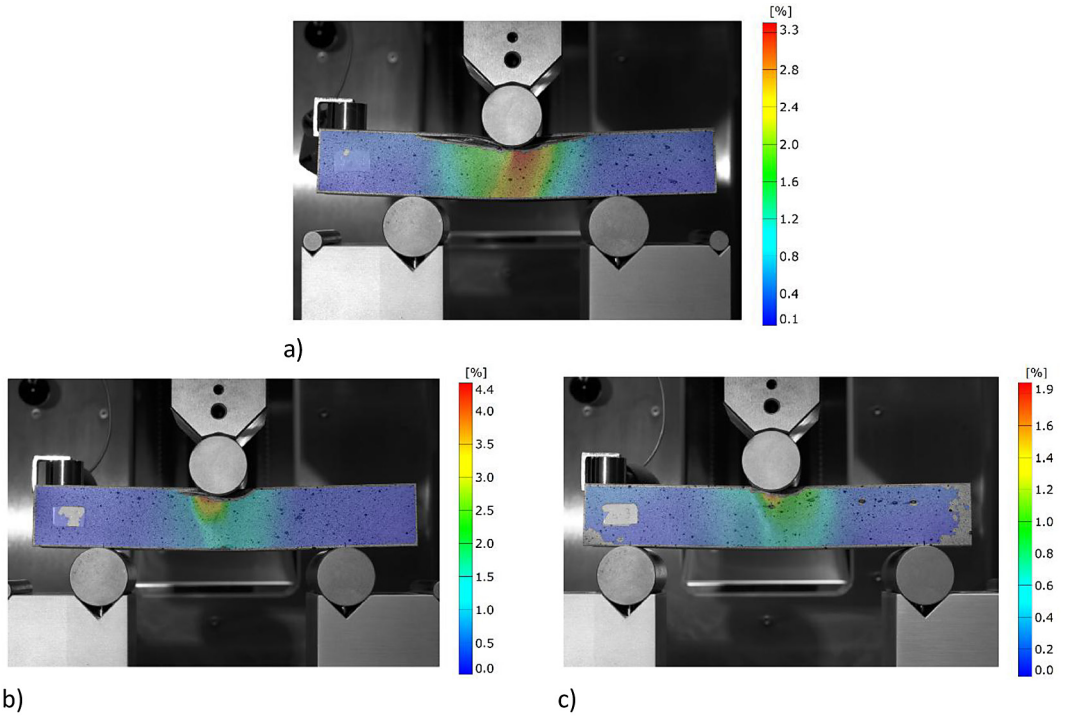

Figure 9. Deformations registered using digital image correlation: a) specimen Sa-1, b) specimen Sa-2, c) specimen Sa-3

digital microscopy. The use of a digital microscope allowed for the observation of the damaged areas – with precise highlighting of the forms of damage to the composite material. For this purpose, the additional depth of field function was used - which enabled a more thorough observation of the defects occurring in the damaged area. In addition, an observation was made at an additional tilt angle of the microscope head of 5° to the edge of the structure where the dominant damage occurred – in order to visualize the damage that had occurred on two surfaces of the composite. A 20x zoom was used during the recording of the damage areas – this was sufficient to capture the main defects in the area under investigation. Figure 10 shows the result of the registered damage areas using digital microscopy.

The research carried out using digital microscopy confirmed that the most extensive and complex damage area was observed in the Sa-1 specimen, where the support spacing was the smallest – 100 mm. The area with the smallest damage was the damage area of the Sa-3 specimen, where the support spacing was the highest – 150 mm. The complex nature of the damage was characterized by both fiber fracture and delamination, which will be analyzed in more detail in further research on composite profiles with different composite material layups. The complex character of damage resulting from the three-point bending phenomenon is shown in Figure 11.

Graphical presentation of the damage area for the Sa-1 specimen is shown for a case 1 (0° of tilt angle of the microscope head relative to the specimen) and for a case 2 (90° of tilt angle of the microscope head relative to the specimen) (Fig. 11). Case 2 shows the surface that was directly subjected to load (top surface) – where fracture of layers and fibers was observed at the edge of the structure (naturally, the damage occurred symmetrically on the second edge within the observed surface). Case 1 shows the surface observed during experimental tests (front

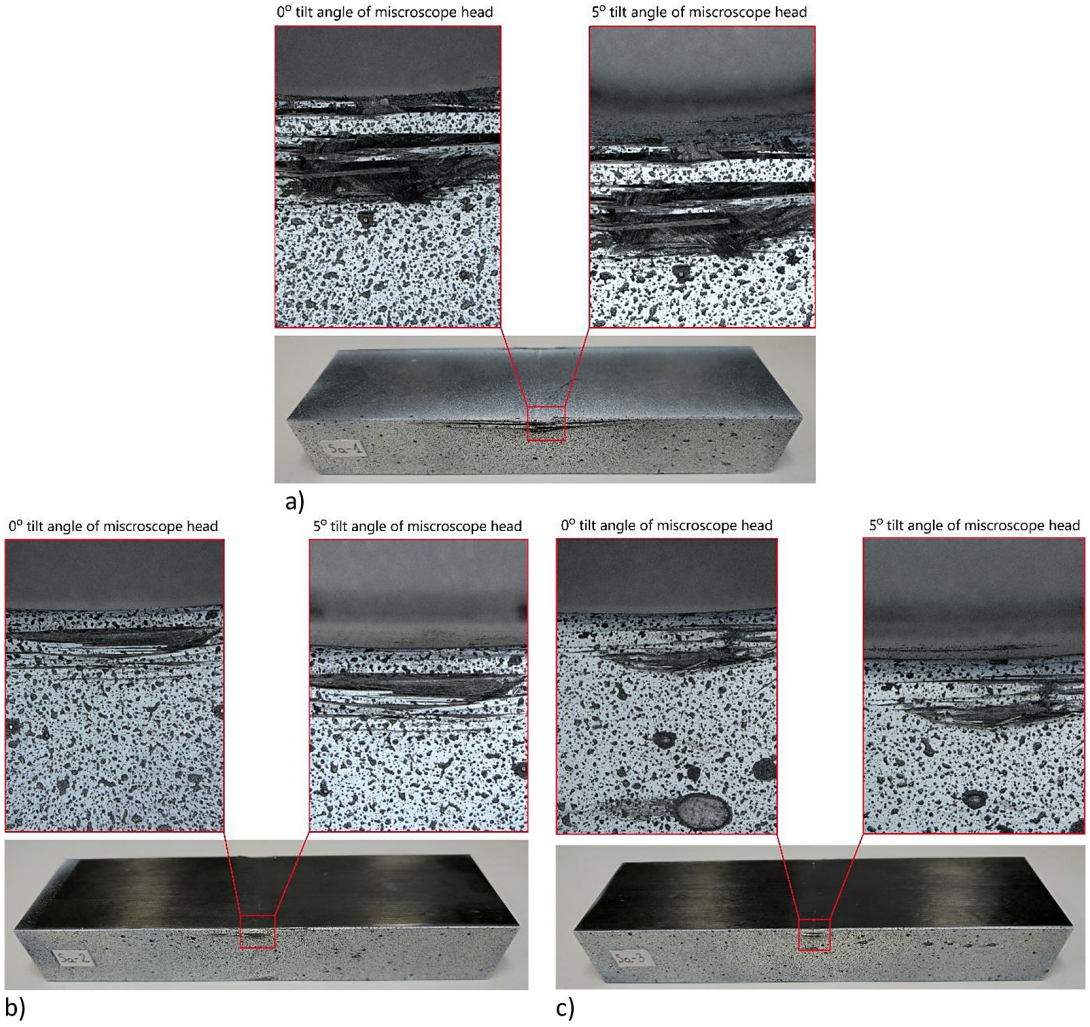

Figure 10. Damage areas presented using digital microscopy: a) specimen Sa-1, b) specimen Sa-2, c) specimen Sa-3

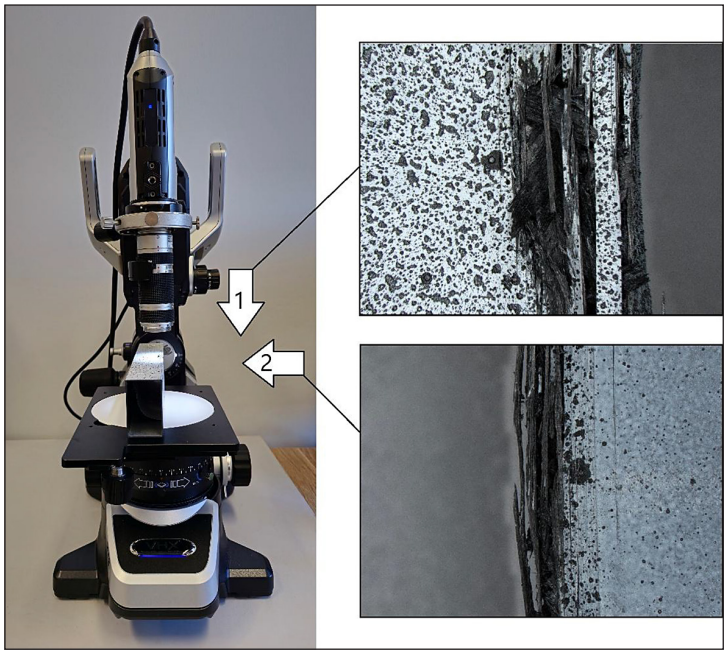

Figure 11. Area of damage at different tilt angles of the microscope head (0° and 90°) – Sa-1 specimen: 1 – indicates the direction of observation (tilt angle of the head 0°), 2 – indicates the direction of observation (tilt angle of the head 90°)

surface) – where its behavior was analyzed using an optical deformation measurement system. In addition, a graphical visualization of the depth of the damage within the 3D view is shown on the example of specimen Sa-1 in the damage area (Fig. 12). This paper constitutes an introduction to the interdisciplinary research activities in the field of possibilities of analyzing and assessing the damage to composite structures. In subsequent publications, more in-depth research results will be presented, especially in the context of the experimental research techniques used,

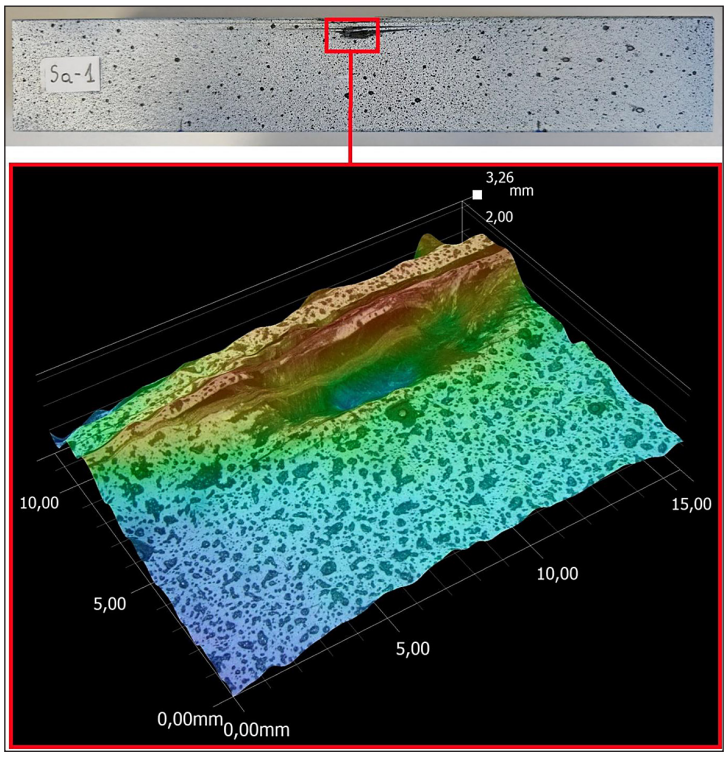

Figure 12. 3D visualization of the damage area of the Sa-1 specimen

as well as an assessment of the impact of other laminate layups on the load-carrying capacity of the structure. In addition, it is planned to develop advanced FEM-based numerical models enabling the simulation of the three-point bending phenomenon with the assessment of loss of load-carrying capacity in the Abaqus program.

CONCLUSIONS

The research provided preliminary information on the behavior of thin-walled three-point-bending composite columns, using several interdisciplinary research techniques. The damage to the composite material resulting from the research activities was assessed, and the following conclusions were formulated:

- Changing the support spacing had a significant impact on the load-carrying capacity of the structure (the limit load was 1.13 times higher for the minimum support spacing of 100 mm than for the maximum support spacing of 150 mm).
- For the composite lay-up used, an almost linear relationship was observed between the decrease in limit load and the increase in support spacing.
- The use of acoustic emission made it possible to determine the intensity of the progressive damage to the bending structures, while the use of a digital 2D image correlation system enabled a graphical assessment of material strain, as well as digital microscopy, which allowed for a graphical assessment of the level of material structure damage.

This study represents the initial stage of research activities in the context of evaluating composite material damage. The paper presents research possibilities leading to the evaluation of composite material damage, using the research devices presented in the paper. The preliminary studies of the bending phenomenon of thin-walled composite structures with closed cross-sections provide information on the possibilities resulting from the use of several research methods to test the load-carrying capacity of composite structures under conditions of variable support spacing within three-point bending tests. In particular, the use of the acoustic emission method and the more detailed investigation of the behavior of the flexural behavior of composite structures in the case of several types of acoustic signals will enable a broader view of the assessment of the complex failure phenomenon.

Acknowledgements

The research was conducted under project No. 2021/41/B/ST8/00148, financed by the National Science Centre, Poland.

REFERENCES

1. Fascetti A, Feo L, Nistic N, Penna R. Web-flange behavior of pultruded GFRP I beams: a lattice model for the interpretation of experimental results. Composites Part B Eng, 2016;100:257–269.
2. Berardi VP, Perrella M, Feo L, Cricrì G. Creep behavior of GFRP laminates and their phases: experimental investigation and analytical modeling. Composites Part B Eng, 2017;122:136–144.
3. Kubiak T, Kolakowski Z, Swiniarski J, Urbaniak M, Gliszczynski A. Local buckling and post-buckling of composite channel-section beams – numerical and experimental investigations. Composites Part B Eng, 2016;91:176–188.
4. Rozylo P. Experimental-numerical test of open section composite columns stability subjected to axial compression. Arch. Mater. Sci. Eng., 2017;84(2):58–64.
5. Kolanu NR, Raju G, Ramji M. A unified numerical approach for the simulation of intra and inter laminar damage evolution in stiffened CFRP panels under compression. Composites Part B, 2020;190:107931.
6. Banat D, Mania RJ. Failure assessment of thin-walled FML profiles during buckling and postbuckling response. Compos Part B Eng 2017;112:278–289.
7. Rozylo P. Failure phenomenon of compressed thin-walled composite columns with top-hat cross-section for three laminate lay-ups. Compos Struct., 2023;304:116381.
8. Rozylo P, Debski H. Failure study of compressed thin-walled composite columns with top-hat cross-section. Thin-Walled Struct., 2022;180:109869.
9. Li ZM, Qiao P. Buckling and postbuckling behavior of shear deformable anisotropic laminated beams with initial geometric imperfections subjected to axial compression. Engineering Structures, 2015;85:277–292.
10. Madukauwa-David ID, Drissi-Habti M. Numerical simulation of the mechanical behavior of a large smart composite platform under static loads. Composites Part B Eng 2016;88:19-25.
11. Gliszczynski A, Kubiak T. Load-carrying capacity of thin-walled composite beams subjected to pure bending. Thin-Walled Struct, 2017;115:76–85.
12. Kazmierczyk F, Urbaniak M, Swiniarski J, Kubiak T. Influence of boundary conditions on the behaviour of composite channel section subjected to

pure bending – Experimental study. Compos Struct, 2022;279:114727.

13. Banat D, Mania RJ, Degenhardt R. Stress state failure analysis of thin-walled GLARE composite members subjected to axial loading in the post-buckling range. Composite Structures, 2022;289:115468.
14. Banat D, Mania RJ. Damage analysis of thin-walled GLARE members under axial compression – Numerical and experiment investigations. Compos. Struct, 2020;241:112102.
15. Li W, Cai H, Li C, Wang K, Fang L. Progressive failure of laminated composites with a hole under compressive loading based on micro-mechanics. Adv. Compos. Mater, 2014;23:477–490.
16. Hu H, Niu F, Dou T, Zhang H. Rehabilitation effect evaluation of CFRP-lined prestressed concrete cylinder pipe under combined loads using numerical simulation. Mathematical Problems in Engineering, 2018;2018:3268962.
17. Gliszczynski A, Czechowski L. Collapse of channel section composite profile subjected to bending, Part I: Numerical investigations. Compos Struct, 2017;178:383–394.
18. Jakubczak P, Gliszczynski A. Bienias J, Majerski K. Kubiak T. Collapse of channel section composite profile subjected to bending Part II: Failure analysis. Compos Struct, 2017;179:1–20.
19. Rozylo P. Failure analysis of beam composite elements subjected to three-point bending using advanced numerical damage models. Acta Mech. Autom., 2023;17:133–144.
20. Heidari-Rarani M, Sayedain M. Finite element modeling strategies for 2D and 3D delamination propagation in composite DCB specimens using VCCT, CZM and XFEM approaches. Composites Part C: Open Access, 2020;2:100014.
21. Camanho PP, Davila CG, de Moura MF. Numerical simulation of mixed-mode progressive delamination in the composite materials, Journal of Composite Materials, 2003;37(16):1415–1438.
22. Ribeiro ML, Vandepitte D, Tita V. Damage model and progressive failure analyses for filament wound composite laminates. Appl. Compos. Mater, 2013;20:975–992.
23. Rozylo P, Debski H. Stability and load carrying capacity of thin-walled composite columns with square cross-section under axial compression. Compos Struct., 2024;329:117795.
24. Rozylo P. Limit states of thin-walled composite structures with closed sections under axial compression. Composites Part B Eng, 2024;287:111813.
25. Rozylo P, Rogala M, Pasnik J. Buckling analysis of thin-walled composite structures with rectangular cross-sections under compressive load. Materials, 2023;16:6835.
26. Rozylo P, Rogala M, Pasnik J. Load-carrying capacity of thin-walled composite columns with rectangular cross-section under axial compression. Materials 2024;17:1615.
27. Huang Y, Sultan M.T.H, Shahar F.S, Grzejda R, Łukaszewicz A. Hybrid fiber-reinforced biocomposites for marine applications: A review. J. Compos. Sci., 2024;8:430.
28. Huang Y., Sultan M.T.H., Shahar F.S., Łukaszewicz A., Oksiuta Z., Grzejda R. Kenaf fiber-reinforced biocomposites for marine applications: A review. Materials, 2025;18:999.
29. PN-EN ISO 527–5:2010; Tworzywa Sztuczne—Oznaczanie Właściwości Mechanicznych Przy Statycznym Rozciąganiu – Część 5: Warunki Badań Kompozytów Tworzywowych Wzmocnionych Włóknami Jednokierunkowo. The Polish Committee for Standardization: Warsaw, Poland, 2010.
30. ASTM D3039; Standard Test Method for Tensile Properties of Polymer Matrix Composite Materials. ASTM International: West Conshohocken, PA, USA.
31. PN-EN ISO 14129:2000; Kompozyty Tworzywowe Wzmocnione Włóknem – Oznaczanie Naprężenia Ścinającego i Odpowiadającego Odkształcenia, Modułu Ścinania i Wytrzymałości Podczas Rozciągania pod Kątem ±45°. The Polish Committee for Standardization: Warsaw, Poland, 2010.
32. ASTM D3518; Standard Test Method for In-Plane Shear Response of Polymer Matrix Composite Materials by Tensile Test of a ±45° Laminate. ASTM International: West Conshohocken, PA, USA.
33. PN-EN ISO 14126:2002; Kompozyty Tworzywowe Wzmocnione Włóknem – Oznaczanie Właściwości Podczas Ściskania Równolegle do Płaszczyzny Laminowania. The Polish Committee for Standardization: Warsaw, Poland, 2010.
34. ASTM D 3410; Standard Test Method for Compressive Properties of Polymer Matrix Composite Materials with Unsupported Gage Section by Shear Loading. ASTM International: West Conshohocken, PA, USA.
35. Rozylo P, Smagowski W, Pasnik J. Experimental research in the aspect of determining the mechanical and strength properties of the composite material made of carbon-epoxy composite. Advances in Science and Technology Research Journal, 2023;17(2):232–246.
36. Hodgkinson J.M. Mechanical Testing of Advanced Fibre Composites. Woodhead Publishing Ltd., Cambridge, 2000.
37. Ramkumar R., Rajaram K., Saravanan P., Venkatesh R., Saranya K., Jenaris D.S. Determination of mechanical properties of CFRP composite reinforced with Abaca and Kenaf fibres. Mater. Today: Proc. 2022;62:5311–5316.